1967

An investigation of the effect of a constant electric field on the diffusion of gold in silicon

Roger D. Peterson
Lehigh University

AN INVESTIGATION OF THE EFFECT OF A CONSTANT ELECTRIC FIELD ON THE DIFFUSION OF GOLD IN SILICON

by

Roger Deane Peterson

A Thesis

Presented to the Graduate Faculty

of Lehigh University

in Candidacy for the Degree of

Master of Science

Lehigh University

1967

CERTIFICATE OF APPROVAL

This thesis is accepted and approved in partial fulfillment of the requirements for the degree of Master of Science.

18 May 1967
Date

Walter C. Hahn, Jr.
Professor in Charge

J. F. Elliott
Chairman of the Department of
Metallurgy and Materials
Science

ACKNOWLEDGEMENTS

The author wishes to express sincere appreciation to Dr. W. C. Hahn, Jr. for his guidance during the course of this investigation and for helpful suggestions in the preparation of the text. Sincere appreciation is also expressed to the Western Electric Company for sponsoring the graduate studies of which this thesis is a part. Grateful acknowledgement is made to Mr. M. J. Brown of the Physics Laboratory and Mr. C. W Henderson, Research Leader, Engineering Research Center, for their technical guidance and assistance in making necessary equipment available for this investigation. Appreciation is also expressed to Mr. P. B. O'Connor, Bell Telephone Laboratories, for the design of the lapping device and assistance in computer programming.

TABLE OF CONTENTS

LIST OF FIGURES

ABSTRACT

The effect of a constant electric field on the diffusion of gold into low dislocation density single crystal silicon was studied at normal diffusion temperatures using radioactive tracer techniques. Diffusion was found to occur as a two stream process consisting of free interstitials and trapped substitutionals. The diffusion coefficients for both streams are presented along with the mobilities of both gold ions and vacancies. The simultaneous effect of temperature on these parameters leads to the conclusion that gold diffuses as a positive ion below 1550^{o}K and as a negative ion above this temperature.

I. INTRODUCTION

A. Introductory Discussion

During the manufacture of some electronic circuit devices a number of diffusion processes are employed to give desired impurity concentrations or bulk properties.

One of these processes, in the production of high speed switching diodes, consists of diffusing gold into semi-conductors to reduce minority carrier lifetime. Gold conveniently furnishes recombination centers both as an acceptor and as a donor. Because the energy levels are deep-lying, however, any compensation is not, in general, one for one. Recombination centers are lattice distortions causing free current carriers to lose energy and become bound in the lattice. As a scattering center, gold lowers the mobility of current carriers by reducing their lifetime, which also tends to increase the measured resistivity of the material. This is the important carrier lifetime effect that increases the switching speed of gold doped devices.

This investigation was undertaken with the hope of learning more about the diffusion of gold in silicon by studying the effect of an electric field on the diffusion mechanism.

B. Diffusion Mechanism (From Wilcox and LaChapelle[2])

The diffusion of gold into silicon has been found to be a two stream process by a number of authors including Sprokel[1], Wilcox and LaChapelle[2], and Sprokel and Fairfield[3]. A slow diffusing

species with a relatively high solubility, in this case substitutional gold, and a fast diffusing species, interstitial gold, diffuse simultaneously.

Together, these two diffusion mechanisms produce a non-Fickian concentration profile because individual atoms may switch from one stream to the other. Even though it is possible to set up boundary conditions for the simplest mathematical models under normal Fickian diffusion, the data may be very difficult to evaluate. In this system, in addition to the two stream process, the very low solubilities of both substitutionals and interstitials control the surface boundary conditions at least during the initial diffusion. Although a substitutional may enter the interstitial stream at any time, an interstitial atom cannot enter a lattice site unless that site is vacant.

Dash[4], in his study of dislocation climb in silicon, observed that the number of vacancies in the bulk of the crystal was very low even at high temperature. He then diffused gold into the crystal and noted climb in the dislocations. Thus dislocations provide sites for interstitial atoms to enter lattice sites. Thus there is a set of conditions such that the speed at which vacancies enter from the surface determines when and where interstitials may switch to substitutionals.

Wilcox and LaChapelle[2] have concluded that four different and distinct diffusion coefficients exist in this system. This is not to imply that only one diffusion mechanism occurs at one time; it

is in fact typical to have three mechanisms operating simultaneously.

Assuming that other factors determine the diffusing temperature of interest, as is the case here, the three variables controlling the dominant shape and speed of diffusion, assuming an infinite crystal, are time, surface concentration, and crystal perfection. The surface concentration and time primarily control the shape, i.e., gaussian or error function; whereas the crystal perfection determines the speed of diffusion.

If crystals with low dislocation density (1000 etch pit counts per square cm) are brought up to a relatively high temperature (greater than 1100^{o}C), three reactions occur at the surface that has gold deposited on it. (1) Gold atoms enter the crystal as interstitials; (2) Gold atoms enter the crystal as substitutionals; (3) Vacancies enter the crystal. Since the solubility of both substitutional and interstitial gold is very low in silicon, the equilibrium concentrations are very quickly reached near the surface. At these temperatures, the movement of substitutionals may be disregarded, as a first approximation, since the diffusion coefficient is much less than that for interstitials and vacancies and as will be shown the equilibrium concentration of substitutionals is reached through a mechanism other than substitutional diffusion. If the movement of vacancies into the crystal is momentarily disregarded and the equilibrium concentration of interstitials is maintained at the surface, the source will appear to be infinite. Thus along with the low dislocation assumption this set of conditions would

produce an error function distribution controlled by the diffusion coefficient for interstitials. Thus, because of the speed of interstitial diffusion, a tail may be expected on any other distribution.

Vacancies are diffusing in from the surface at the same time that the interstitials are diffusing but substantially slower. When an interstitial atom combines with a vacancy to produce a substitutional, the atom is effectively removed from the diffusing stream. Thus a distribution of substitutional atoms appears in addition to the pure interstitial distribution.

This additional distribution is indirectly controlled by the diffusion coefficient of vacancies.

If the reaction

$$Au_i + V = Au_{sub} \qquad (1)$$

is in equilibrium at all times, it may be stated thus:

$$C_{sub}/C_iC_v = K \qquad (2)$$

Where K is an equilibrium constant which is a function of temperature alone. Because of the speed at which the interstitials are moving in the region where an appreciable number of vacancies are present, to the first approximation $C_i = (C_i)_s$; the interstitial concentration still equals the maximum solubility of interstitials, thus

$$C_{sub} = (C_i)_s KC_v \qquad (3)$$

The expression for the vacancy diffusion is then

$$D_v \frac{\partial^2 C_v}{\partial x^2} = \frac{\partial C_v}{\partial t} + \frac{\partial C_{sub}}{\partial t} \qquad (4)$$

or using equation (3)

$$D_v \frac{\partial^2 C_v}{\partial x^2} = (1 + K(C_i)_s) \frac{\partial C_v}{\partial t} \qquad (5)$$

If it is assumed surface cracks and imperfections provide an infinite source of vacancies, (the crystals are butted together in this investigation) then the surface concentration is constant and equal to the maximum solubility of vacancies. The solution is then

$$C_v = (C_v)_s \operatorname{erfc}\left\{ x/2\sqrt{D_{eff} t} \right\} \qquad (6)$$

where

$$D_{eff} = D_v/(1 + K(C_i)_s)$$

or since equation (3) holds at all concentrations,

$$D_{eff} = (C_v)_s D_v / ((C_v)_s + (C_{sub})_s) \qquad (7)$$

Because it is impossible to detect vacancies or a single species, the experimentally determined distribution will be:

$$C = C_i + C_{sub} = (C_i)_s \operatorname{erfc}\left\{ x/2\sqrt{D_i t} \right\} + (C_{sub})_s \operatorname{erfc}\left\{ x/2\sqrt{D_{eff} t} \right\} \qquad (8)$$

Fortunately $(C_{sub})_s$ is greater than $(C_i)_s$ and D_i is greater than D_{eff}, thus the initial distribution is primarily vacancy controlled; whereas the tail is interstitially controlled. It is important to note that two conditions must be met for this solution to hold. The deposited gold must maintain the maximum interstitial gold

concentration at the surface and the effective bulk vacancy concentration (due to dislocations) must be much smaller than the maximum interstitial gold concentration.

It is quite simple to determine if the first condition is met. If the surface concentration is insufficient, the initial distribution will change from an error function to a gaussian shape.

Proof of the second condition is somewhat more difficult to determine. First the data points in the tail region must fit an error function, that is, they must be controlled by a single diffusion mechanism. If this condition is met, then one of two mechanisms is controlling the diffusion. If the maximum solubility of interstitials, $(C_i)_s$, is much larger than the bulk concentration of vacancies, $(C_v)_b$, the initial conditions are met. But if $(C_v)_b$ is larger than $(C_i)_s$, equation (2) becomes

$$C_{sub} = (C_v)_b \, KC_i \tag{9}$$

and the diffusion equation becomes

$$D_i \frac{\partial^2 C_i}{\partial x^2} = \frac{\partial C_i}{\partial t} + \frac{\partial C_{sub}}{\partial t} \tag{10}$$

which, assuming the surface condition is met, has the solution

$$C_i = (C_i)_s \, \mathrm{erfc} \left\{ x/2\sqrt{D_{eff} t} \right\} \tag{11}$$

where

$$D_{eff} = (C_i)_s \, D_i \, / \, ((C_i)_s + (C_{sub})_s) \qquad (12)$$

At all the temperatures of interest this ratio is on the order of one tenth[2].

Thus if the diffusion coefficient of the tail region is near the value calculated by Wilcox and LaChapelle[2] for interstitials and the tail region is best fitted with an error function, the sole diffusion mechanism is interstitial. The importance of this conclusion will become apparent in the following sections.

It is possible to measure D_{sub} directly at low temperatures if the annealing time is very long. The effective diffusion coefficient controlled by vacancies is very dependent on temperature.[2]

The last case to be considered consists of crystals with very high dislocation density. If the effective bulk vacancy density is comparable to the equilibrium concentration of vacancies the conditions are identical to those presented in equation (9) and the effective diffusion coefficient is again

$$D_{eff} = (C_i)_s \, D_i / ((C_i)_s + (C_{sub})_s) \qquad (13)$$

No tail exists in this distribution.

C. <u>The Effect of an Electric Field and High Current Density</u>

An electric field in metals causes the motion, not only of free electrons, but also of ions. An impurity ion moves under the influence of two forces: the external electric field and a

force acting on the ion due to electrons. The force due to the scattering of electrons causes the ions to move against the field.

In 1953, Haeffner[5] discovered the isotopic separation of mercury ions by a constant current, and this effect was later established for a number of other metals.

In order to explain the qualitative rules for the motion of impurity ions, Skaupy[6] assumed that they can have an effective charge different from the ions of the metal. In addition, Skaupy introduced the concept of mutual friction of the electrons against the ions. For ions belonging to the metal itself, this frictional force is equilibrated by the action of the external field on the ion. If impurity ions decrease the electrical conductivity of the metal, then they experience a larger frictional force than the ions of the metal and vice versa. These considerations lead to the following rule[7]. If impurity ions decrease the electrical conductivity, then they move toward the anode. If they increase it, they move toward the cathode. This rule is basically in agreement with experiments on the motion of ions in mercury.

Fiks[7] states that a weakness of all the early ideas consists in the fact that they either do not consider the interaction of electrons with ions in general and are therefore incorrect, or they consider this interaction formally--by the introduction of a coefficient of friction.

The interaction of electrons with ions can be examined logically only in the framework of the electron theory of metals[7].

To begin with, the theory should establish a connection among the effective mobility of a ion, the coefficient of diffusion, the electrical properties of the metal, and the physical parameters of the ion which characterize its interaction with electrons.

Fiks[8] proceeded to calculate a theoretical force on an ion from both the electrical field and the collisions of the electrons with the ion, much like calculations for electron lifetime in conductivity theory. His results are:

$$F = e\,E\,(1-nl\,\sigma_i) \tag{14}$$

where E is the intensity of the electric field, l is the mean free path of an electron (assumed to be independent of the energy), σ_i is the electron scattering cross section of ions, e is the charge on the electron and n is the concentration of electrons. If we define the true mobility as

$$\mu_o = v/F \tag{15}$$

where v is the velocity of the ion and the effective mobility as

$$\mu_{eff} = v/e\,E \tag{16}$$

we find that

$$\mu_{eff} = \mu_o(1 - nl\,\bar{\sigma}_i) \tag{17}$$

where $\bar{\sigma}_i$ is the average scattering cross section over all energies.

The scattering of electron by a coulomb center in a semiconductor was considered by Brooks[9], who took into account the

space-charge effect. His conclusions give the following expression for the average scattering cross section to the first approximation.

$$\bar{\sigma}_i = 2.5 \times 10^{-11} \left(\frac{300}{T}\right)^2 B/D^2 \qquad (18)$$

Where D is the dielectric constant T is the temperature, and B is a function almost independent of T. That is, B varies by a factor of two when the temperature varies from $300^{o}K$ to $1500^{o}K$.

If the temperature variation of the mean free path of electrons and the concentration of electrons in a semiconductor are taken into account, the temperature at which the scattering term becomes equal to the external electric field term can be calculated. At this temperature one would expect the effective mobility of a positive ion to be zero.

In the case of gold in silicon, Fiks[8] calculated this temperature to be $1600^{o}K$. At about the same time Boltaks et al.[10] studied the electro-diffusion of gold in silicon and noted a change in sign of the mobility at $1553^{o}K$. However, in light of the fact that the diffusion coefficients reported by Boltaks were analyzed by Wilcox and LaChapelle[2] to be vacancy diffusion controlled, this investigation of the same system was undertaken.

When the effects of an electric field are considered in the diffusion mechanism, for example in the interstitial case, the following equation holds to the first approximation[10].

$$C_i = (C_i)_s \operatorname{erfc} \left\{ (x - \mu_{eff} E t) \,/\, 2\sqrt{D_i t} \right\} \qquad (19)$$

The fact that interstitial atoms are lost to the substitutional stream and the source remains at x = 0 are not considered in this approximation.

If the force on ions due to electrons is in reality much too small at this temperature to be detected, the mobility of the interstitial atoms should conform well with the Einstein relation, where k is Boltzmann's constant, T is the temperature, and q is the charge on the ion.

$$D/\mu = KT/q \tag{20}$$

II. EXPERIMENTAL PROCEDURE

The complications of the diffusion mechanism required the selection of a single system to be studied and conditions closely controlled to maintain only one mechanism. To study the effects of impurity ion and electron interaction, a mechanism controlled by the concentration of these ions and independent of surface conditions should be used. Three systems would meet these requirements: (1) A pure substitutional with maximum substitutional solubility maintained at the surface, (2) An interstitial diffusion controlled in a crystal with the equilibrium number of vacancies in the bulk with maximum interstitial solubility maintained at the surface, (3) A pure interstitial with maximum interstitial solubility maintained at the surface. The first of these may be eliminated because of the great difficulty in attaining it at the temperatures of interest; i.e., it is the slowest mechanism and thus the concentration profile is really the sum of three mechanisms. The second may be eliminated because of the difficulty of proving the equilibrium number of vacancies condition is met; i.e., the dislocation density in the bulk of the crystal acts the same as though the equilibrium number of vacancies existed in the crystal. Since vacancies diffuse slower than interstitials at all temperatures it is difficult if not impossible to establish the vacancy concentration before diffusing. The third, although difficult to attain, was determined to be the system to be studied.

In light of the foregoing discussion the following experimental conditions were used.

1. The diffusing crystals were of very high purity.
2. The diffusing crystals had very few imperfections.
3. The diffusing time and surface concentration were controlled so that the maximum solubility of interstitials was maintained at the surface.
4. Only the interstitial diffusion controlled tails were used in mobility calculations for gold ions.

The concentration of gold in the silicon bars was determined by the radioactive tracer technique. Due to a lack of knowledge of all the ramifications in the diffusion of gold in silicon the optimum radioactive isotope was not selected and both time and availability of the optimum material prevented a change. The dominating condition is the very low solubility of interstitial gold. Thus the need for a better signal to noise ratio dictated the need for an isotope with a high specific activity. Gold 195 was used, carrier free, as the tracer and gave activities of the same magnitude as the background count in the all important interstitial diffusion controlled region (See Appendix 3). The selection of a specific isotope affects the scattering cross section, but Haeffner's[5] results indicate the variation between isotopes of a given element is small.

The dislocation density on the diffusing surface of each crystal was determined by an etch pit count after a hard acid etch. A drop of radioactive tracer, in the form of dissolved

gold chloride, was then placed on the diffusing surface of each of two crystals and allowed to evaporate at room temperature.

The diffusing surfaces were then butted together and placed in a special holder (Figure 1). The holder was placed in a gas tight aluminum oxide or quartz tube (Figure 2) which was flushed with purified argon gas during the annealing run. The holder was moved to the ends of the tube so that only the tungsten electrode rods touched the crystals. Preheating the tube and crystals in a standard tube furnace to 550^{o}C created sufficient intrinsic carriers to allow resistive heating to begin. A power supply with .1% current control applied a direct current through the electrodes and crystals. The tube was immediately removed and allowed to radiate in still air. When the diffusion run was completed, the current was removed and the tube allowed to cool by radiation and conduction through the water cooled electrodes.

Two calibration runs were required, the first for temperature versus current and the second for temperature variation. These runs were made using crystals that did not meet the dislocation density requirement. Temperature could not be measured during a diffusion run with a thermocouple, since any object near the crystal outside surface caused extreme localized heating (the crystal locally melted during initial attempts). Surface temperature was in fact misleading since temperature from center to outer surface varied 140^{o}C. The calibration consisted of placing a thin tungsten slice between two calibration crystals. A small hole

in the edge of the slice accommodated a tungsten vs. tungsten-rhenium thermocouple (Appendix 2). A simulated diffusion run was made except that the current was continually increased until an increase in current produced no increase in temperature. Later visual evidence confirmed the fact that internal melting had taken place in the crystals, thus the temperature readings were corrected to the melting point of silicon. Temperatures reported in this paper are in reference to the center of the crystal. The corrected temperature was used to determine the theoretical intrinsic resistivity[11]. The electric field in the diffusion region of interest was then calculated using the measured electric current. Variations in temperature were determined by monitoring the voltage across the diffusing crystals. These readings indicate that for all temperatures the time required for heating from 550°C to the diffusion temperature was less than three seconds, the variation in temperature during any run was $\pm$ 6°C, and the cooling time, determined by intrinsic resistivity, was less than seven seconds to 900°C

No material was normally removed from the sides of the crystals before lapping, as is the standard practice, for the following reasons: the butted crystal inhibited the evaporation, the surface temperature is much lower, and most important, test samples indicated no change before and after side removal.

The crystals were mounted on a hand lapping device (Figure 3) (Appendix 1) to maintain parallelism and ground using standard 240 grit paper. The crystal mount was weighed between lapping to

determine depth and the activity of the grindings determined using a scintillation counter.

A computer program determined the best fit error function for both the tail and surface region, calculated confidence intervals, determined diffusion coefficients and calculated effective mobility.

III. EXPERIMENTAL RESULTS

A. Data

The following table contains the data accumulated during the lapping and counting procedure performed after the diffusion anneal. The density of silicon was used to determine section length from the weight of the slice. The text continues on page 28.

TABLE I

EXPERIMENTAL DATA

Section Weight (mg)	Number of Counts (c/hr)	Section Depth (cm)	Activity (c/hr/micron)
Run number 1 (40 amperes for 10 minutes) 1512°K			
Anode			
8.1	70103	0.00697	496.0
4.1	22812	0.0175	312.0
5.5	24093	0.0257	245.0
14.1	18051	0.0426	70.8
10.1	8963	0.0634	35.2
10.6	3024	0.0812	11.8
11.5	1821	0.100	4.85
Cathode			
9.9	75486	0.00851	437.0
6.0	28355	0.0222	272.0
6.5	24493	0.0329	211.0
13.2	22584	0.0499	95.5
10.0	8462	0.0698	44.5
9.8	2521	0.0868	9.96
10.7	1504	0.105	3.59

TABLE I (cont.)

EXPERIMENTAL DATA

Section Weight (mg)	Number of Counts (c/hr)	Section Depth (cm)	Activity (c/hr/micron)
Run Number 2 (50 amperes for 15 minutes) 1578°K			
Anode			
9.3	140932	0.00800	882.0
11.8	61427	0.0261	302.0
12.8	37582	0.0473	170.0
11.0	17698	0.0678	93.6
12.0	7203	0.0875	34.8
12.3	2911	0.108	13.7
11.4	1098	0.129	5.6
Cathode			
10.7	151621	0.00920	822.0
13.9	73520	0.0304	308.0
10.0	36181	0.0509	210.0
12.3	23912	0.0701	113.0
13.3	9180	0.0921	40.1
9.4	2591	0.112	15.9
11.6	743	0.130	3.7
Run Number 3 (55 amperes for 10 minutes) 1607°K			
Anode			
2.6	64388	0.00112	2880.0
8.7	33729	0.00972	225.0
9.8	29330	0.0256	174.0
8.2	14710	0.0411	104.0
8.1	9664	0.0551	69.3
8.4	5958	0.0693	41.3
8.7	3514	0.0840	23.5
9.5	2436	0.0996	14.9
9.3	1568	0.116	9.8
9.2	1230	0.131	7.8
9.9	1310	0.148	7.7
9.8	910	0.165	5.4
10.2	948	0.182	5.4
10.7	776	0.200	4.2
19.2	1296	0.226	3.9
16.2	894	0.256	3.2
18.1	974	0.286	3.1
20.9	676	0.319	1.9

TABLE I (cont.)

EXPERIMENTAL DATA

Section Weight (mg)	Number of Counts (c/hr)	Section Depth (cm)	Activity (c/hr/micron)
Run Number 3 (55 amperes for 10 minutes) 1607°K (cont.)			
Cathode			
3.0	53066	0.00258	1029.0
9.7	38678	0.0135	232.0
9.0	26622	0.0296	172.0
8.3	17604	0.0445	123.0
10.7	12710	0.0608	69.0
9.1	5800	0.0778	37.1
8.8	3436	0.0932	22.7
9.3	2362	0.109	14.7
8.1	1308	0.124	9.4
8.3	1060	0.138	7.4
10.6	1204	0.154	6.6
12.1	1080	0.174	5.2
8.0	496	0.190	3.6
13.8	718	0.210	3.0
17.0	770	0.236	2.6
17.6	500	0.266	1.6
17.0	430	0.296	1.5
Run Number 4 (45 amperes for 15 minutes) 1548°K			
Anode			
1.5	35400	0.00129	1372.0
8.2	61060	0.00963	433.0
8.6	37560	0.0241	254.0
10.4	27950	0.0404	157.0
8.4	14800	0.0566	102.0
8.6	2640	0.0712	17.8
10.6	1870	0.0877	10.3
19.5	1640	0.114	4.9
18.0	1360	0.146	4.4
16.0	1250	0.175	4.5
17.3	1150	0.204	3.9
14.7	795	0.231	3.1
15.1	525	0.257	2.0
17.4	421	0.285	1.4
15.4	290	0.313	1.1

TABLE I (cont.)

EXPERIMENTAL DATA

Section Weight (mg)	Number of Counts (c/hr)	Section Depth (cm)	Activity (c/hr/micron)
Run Number 4 (45 amperes for 15 minutes) 1548°K (cont.)			
Cathode			
1.5	37600	0.00129	1457.0
9.7	66400	0.0109	398.0
10.2	42600	0.0280	243.0
9.2	20800	0.0447	131.0
9.2	9460	0.0605	59.8
8.5	2700	0.0758	18.5
17.2	2580	0.0979	8.7
19.9	2260	0.129	6.6
16.4	878	0.161	3.1
19.3	896	0.192	2.7
15.3	775	0.221	2.9
15.8	631	0.248	2.3
15.6	394	0.275	1.5
14.6	223	0.301	.9
15.0	240	0.327	.9
Run Number 5 (35 amperes for 15 minutes) 1476°K			
Anode			
3.1	152000	0.00267	2851.0
5.7	71850	0.0102	733.0
7.5	56300	0.0216	436.0
6.4	33500	0.0335	304.0
6.2	20600	0.0444	193.0
7.1	9180	0.0558	75.2
7.0	6550	0.0679	54.4
8.5	3630	0.0813	24.8
6.7	1190	0.0943	10.3
6.5	1050	0.106	9.4
15.7	1000	0.125	3.7
12.9	550	0.149	2.4
16.2	1000	0.174	3.5
14.5	794	0.201	3.2
14.7	652	0.226	2.5
16.1	884	0.252	3.2
13.8	410	0.278	1.7
15.1	341	0.303	1.3
14.1	208	0.328	.8

TABLE I (cont.)

EXPERIMENTAL DATA

Section Weight (mg)	Number of Counts (c/hr)	Section Depth (cm)	Activity (c/hr/micron)
Run Number 5 (35 amperes for 15 minutes) 1476°K (cont.)			
Cathode			
1.7	98300	0.00146	3362.0
7.0	76000	0.00894	631.0
6.9	51200	0.0209	431.0
7.1	36200	0.0329	296.0
6.5	22400	0.0446	200.0
5.5	11500	0.0550	121.0
7.5	9100	0.0661	70.5
8.1	3960	0.0795	28.4
6.4	1650	0.0920	14.9
6.0	710	0.103	6.9
14.3	1534	0.120	6.2
13.1	892	0.144	3.9
16.0	858	0.169	3.1
15.7	604	0.196	2.2
16.4	608	0.224	2.2
12.8	642	0.249	2.9
12.6	582	0.271	2.7
13.9	420	0.293	1.8
14.3	328	0.318	1.3
13.5	278	0.342	1.2
Run Number 6 (35 amperes for 20 minutes) 1476°K			
Anode			
1.0	6044	0.00086	351.0
7.6	15663	0.00826	120.0
9.1	15650	0.0226	100.0
9.2	10556	0.0384	67.0
10.1	7334	0.0550	42.2
12.2	3768	0.0741	18.0
9.2	970	0.0925	6.1
9.1	340	0.108	2.2
18.1	603	0.132	1.9
17.5	591	0.162	2.0
12.7	450	0.188	2.0
14.8	506	0.212	2.0
15.2	462	0.238	1.8
14.4	236	0.263	.9
17.4	242	0.290	.8

TABLE I (cont.)

EXPERIMENTAL DATA

Section Weight (mg)	Number of Counts (c/hr)	Section Depth (cm)	Activity (c/hr/micron)
Run Number 6 (35 amperes for 20 minutes) 1476°K (cont.)			
Cathode			
1.1	5436	0.000946	288.0
8.3	20990	0.00903	147.0
9.1	15486	0.0240	99.0
8.3	11030	0.0389	77.1
11.8	9260	0.0562	45.6
9.9	3604	0.0745	21.1
10.0	1562	0.0920	9.1
8.4	688	0.108	4.8
17.5	1084	0.130	3.6
14.7	264	0.158	1.0
17.2	304	0.185	1.0
17.1	450	0.215	1.5
14.3	106	0.242	.4
14.9	320	0.267	1.2
18.2	124	0.295	.4
Run Number 7 (40 amperes for 10 minutes) 1512°K			
Anode			
0.9	152100	0.000774	9819.0
5.3	80600	0.00611	884.0
6.6	70100	0.0163	617.0
6.1	41500	0.0273	396.0
6.6	24400	0.0382	215.0
6.5	11900	0.0494	106.0
6.2	5500	0.0604	51.6
7.3	3400	0.0720	27.1
8.5	2180	0.0856	14.9
14.8	2070	0.106	12.1
14.3	2580	0.131	10.5
12.1	1800	0.153	8.6
13.5	1720	0.175	7.4
13.4	1510	0.198	6.6
13.3	1240	0.221	5.4
13.2	1060	0.244	4.7
13.6	840	0.267	3.6

TABLE I (cont.)

EXPERIMENTAL DATA

Section Weight (mg)	Number of Counts (c/hr)	Section Depth (cm)	Activity (c/hr/micron)
Run Number 7 (40 amperes for 10 minutes) 1512°K (cont.)			
Cathode			
1.2	205000	0.00103	9932.0
6.8	110000	0.00791	940.0
6.5	73000	0.0193	654.0
6.6	50300	0.0306	443.0
6.8	26900	0.0421	230.0
7.9	14800	0.0548	110.0
6.9	5500	0.0675	46.5
7.7	3100	0.0801	23.4
7.7	2110	0.0933	15.9
11.9	2408	0.110	11.8
12.9	2330	0.131	10.5
13.8	2030	0.154	8.6
12.9	1700	0.177	7.7
12.7	1500	0.199	6.9
12.2	1290	0.221	6.1
13.4	1100	0.243	4.8
14.1	1060	0.267	4.4
Run Number 8 (65 amperes for 10 minutes) 1668°K			
Anode			
1.0	78750	0.00086	4580.0
14.1	32680	0.0138	134.0
17.4	19040	0.0409	63.5
19.3	11830	0.0725	35.5
19.3	5675	0.106	17.1
21.1	4500	0.140	12.4
17.4	2075	0.174	6.95
12.5	1006	0.199	4.65
11.7	708	0.220	3.52
12.5	666	0.241	3.10
12.7	904	0.263	4.14
21.9	1180	0.292	3.13
14.1	768	0.323	3.17
12.8	684	0.346	3.11
11.5	458	0.367	2.32
14.5	370	0.390	1.48
15.0	260	0.415	1.01

TABLE I (cont.)

EXPERIMENTAL DATA

Section Weight (mg)	Number of Counts (c/hr)	Section Depth (cm)	Activity (c/hr/micron)
Run Number 8 (65 amperes for 10 minutes) 1668°K (cont.)			
Cathode			
2.1	137600	0.00181	3790.0
14.0	37360	0.0167	155.0
20.5	30620	0.0453	86.8
16.1	10250	0.0768	37.2
19.4	7975	0.107	23.9
19.0	3875	0.140	11.9
17.6	2710	0.172	8.95
12.5	1075	0.198	5.02
13.9	1100	0.220	4.60
11.9	1156	0.243	5.67
14.1	1202	0.265	4.95
14.6	960	0.290	3.82
13.7	944	0.314	4.01
13.6	504	0.337	2.15
15.0	578	0.362	2.24
12.7	498	0.386	2.28
14.8	160	0.410	0.63
Run Number 9 (50 amperes for 10 minutes) 1578°K			
Anode			
0.7	37060	0.000602	3080.0
8.3	60680	0.00834	425.0
8.9	46210	0.0231	302.0
8.1	22350	0.0378	161.0
8.1	10216	0.0517	73.2
9.7	5664	0.0670	33.9
8.9	1944	0.0830	12.7
18.0	1776	0.106	5.75
15.3	848	0.135	3.22
16.3	646	0.162	2.30
22.5	598	0.195	1.55
23.6	455	0.235	1.12

TABLE I (cont.)

EXPERIMENTAL DATA

Section Weight (mg)	Number of Counts (c/hr)	Section Depth (cm)	Activity (c/hr/micron)
Run Number 9 (50 amperes for 10 minutes) 1578°K (cont.)			
Cathode			
0.7	43380	0.000602	3605.0
8.4	70620	0.00843	489.0
8.9	49060	0.0233	321.0
9.2	30060	0.0388	190.0
8.5	14108	0.0541	96.4
8.2	6044	0.0684	42.8
8.8	2546	0.0831	16.8
18.2	1840	0.106	5.88
15.5	770	0.135	2.89
17.8	486	0.164	1.59
23.0	249	0.199	0.63
Run Number 10 (25 amperes for 15 minutes) 1407°K			
Anode			
8.2	361400	0.00705	2560.0
7.8	73410	0.0208	547.0
7.1	31940	0.0336	261.0
6.5	13338	0.0453	119.0
7.3	7004	0.0572	55.7
8.5	3950	0.0708	27.0
7.6	1516	0.0846	11.7
13.6	672	0.103	2.87
15.2	500	0.128	1.91
14.0	250	0.153	1.04
16.6	146	0.179	0.51
16.9	160	0.208	0.55
15.7	76	0.236	0.28

TABLE I (cont.)

EXPERIMENTAL DATA

Section Weight (mg)	Number of Counts (c/hr)	Section Depth (cm)	Activity (c/hr/micron)
Run Number 10 (25 amperes for 15 minutes) 1407°K (cont.)			
Cathode			
6.8	390500	0.00584	3330.0
6.7	78250	0.0174	679.0
6.7	41800	0.0290	363.0
7.0	23790	0.0408	198.0
8.0	12648	0.0537	91.6
8.1	5250	0.0675	37.7
6.8	1906	0.0804	16.3
14.7	1556	0.0988	6.17
14.5	330	0.124	1.32
17.4	258	0.151	0.86
16.4	264	0.180	0.94
15.8	228	0.208	0.74
16.2	205	0.237	0.73

B. Analysis

The data in Table I was analyzed by assuming equation (19) holds for the tail region.

$$C_i = (C_i)_s \operatorname{erfc}\left\{(x-\mu_{eff}Et)/2\sqrt{D_i t}\right\} \qquad (19)$$

The best fit error function compliments were used to calculate the diffusion coefficient and the effective mobility at each temperature. The scatter of the data points was used to determine confidence intervals. The calculated values of the interstitial concentration, at the respective depths, were subtracted from the initial data points. The resultant values were fitted with the best fit error function compliment assuming equation (21) holds,

$$C_{sub} = (C_{sub})_s \operatorname{erfc}\left\{(x-\mu_v Et)2\sqrt{D_{eff}t}\right\} \qquad (21)$$

where μ_v is the effective mobility of vacancies and D_{eff} is defined by equation (7). Figures 4, 5, and 6 are examples of the data points and the best fit error function compliments for the anode and cathode concentration profiles separately. The data is plotted as depth versus concentration on a probability scale so that the error function compliments appear as straight lines. The different slopes of the initial concentration profiles is noticeable in all three of the examples indicating the tendency of vacancies to be attracted to the cathode. Figure 4 illustrates the interstitials being attracted to the anode since the temperature of diffusion is above the critical temperature for the mobility of gold ions. Figure 5 is an example of the diffusion profile below the critical temperature

and indicates interstitials are attracted to the cathode. The relatively low diffusing temperature used to obtain the distribution shown in Figure 6, indicates the difficulties of determining the interstitial concentrations when the solubility has decreased to a point near the system noise.

Table II lists the values of the diffusion coefficients, relative solubilities, i.e., the intercepts not corrected for specific activity, and mobilities for each temperature. Figure 7 is an Arrhenius plot for both interstitial and vacancy controlled diffusion coefficients. The lines are those reported by Wilcox and LaChapelle[2] as determined from data over a much larger temperature range. It should be noted that the deviations from line number 3 are in general agreement with data reported in this literature. Figure 8 indicates the temperature dependence of the mobility of gold in silicon. The shape of the curve agrees with the literature[10], but the values are an order of magnitude larger. The calculated values shown were made by substituting the measured diffusion coefficient into Einstein's relationship with an electron charge of plus one at low temperatures and minus one at high temperatures.

The temperature dependence of the mobility of vacancies in silicon is shown in Figure 9. The calculated values shown on the plot were calculated assuming an electronic charge of plus one for vacancies. These calculated values are in error because the ratio $(C_v)_s/((C_s)_s + (C_{sub})_s)$ is not known.

The relative solubilities are shown in Figure 10 versus temperature and are in general agreement with those reported by Trumbore[14].

TABLE II

EXPERIMENTAL ANALYSIS

Run No.	Temperature (^{o}K)	Electric Field (volts/cm)	Diffusion Coefficient		Mobility		Relative Solubility	
			Interstitial Controlled ($cm^2/sec \times 10^5$)	Vacancy Controlled ($cm^2/sec \times 10^7$)	Interstitial Controlled ($cm^2/volt\text{-}sec \times 10^5$)	Vacancy Controlled ($cm^2/volt\text{-}sec \times 10^6$)	Interstitial Controlled (counts/micron-hr)	Vacancy Controlled (counts/micron-hr)
1	1512	0.592	--	12.2±1.0	--	9.32±1.0	--	--
2	1578	0.510	--	14.8±0.7	--	7.19±0.11	--	--
3	1607	0.475	3.86±0.33	19.7±1.3	-15.3±6.9	17.4±2.6	12.5	280.0
4	1548	0.540	2.32±0.39	7.32±0.51	0.897±13.6	3.29±0.49	10.1	539.0
5	1476	0.630	3.19±0.39	6.83±0.26	5.51±7.83	4.15±0.35	6.26	953.0
6	1476	Surface concentration not maintained						
7	1512	0.592	3.54±0.15	8.10±0.24	4.11±5.2	6.90±1.05	20.7	1152.0
8	1668	0.395	5.92±1.08	23.1±1.8	-15.9±19.9	12.6±2.8	15.4	182.0
9	1578	0.510	1.36±0.14	11.4±0.4	-8.92±0.27	3.43±0.75	13.6	582.0
10	1407	0.66	1.44±1.12	4.62±0.23	12.6±2.7	0.67±0.10	7.49	1212.0

IV. CONCLUSIONS AND DISCUSSION

The behavior of the mobility of gold in silicon above the temperature of 1553°K, was explained by Boltaks[10] as a manifestation of the interaction of electrons and ions as predicted by Fiks[8]. While this solution appears plausible, the approximations used in the theory are such that the value of the reversal temperature may very easily be considerably higher than the melting point. The basic omission, as admitted by Fiks, was not considering the entrainment effect of holes. The calculation of equation (17) requires the assumption of complete degeneracy of the electrons as in a metal, whereas the calculation of equation (18), from Brooke, requires the assumption of no degeneracy as in an intrinsic semiconductor (as is the case here). Fiks also assumed that the mean free path varied with temperature according to the theoretical slope for scattering by lattice thermal vibrations. This has not been found experimentally to be the case[15].

There is no reason to expect other characteristics such as maximum solubility and diffusion coefficients to be affected by a large number of drifting carriers. But the mobility of vacancies, since they are charged lattice distortions and thus scattering sites, would be expected to show some reaction although possibly not as great as gold ions.

The slope of the vacancy controlled diffusion, shown in Figure 7, indicates a smaller dependence on temperature in the region

above 1200°C than found by Wilcox and LaChapelle[2]. If this slope were extended to lower temperatures, the predicted values would be grossly different than those observed. Thus, it can be concluded that the slope has changed for one reason or another. This diffusion is controlled by the rate of vacancy diffusion and equilibrium ratio of the number of vacant lattice sites to the number of sites not containing silicon atoms (equation 7). It appears difficult to explain a change in the "activation energy" without a structural change in the silicon, if the nature of the vacancy or gold ion has not changed.

The dip in the plot of the interstitial controlled diffusion coefficient versus temperature is also hard to explain using the entrainment theory (Figure 7). It must be noted that the low signal to noise ratio made accurate measurement difficult in the interstitial region, so that the data has considerable spread. A change from a small positive ion to a large negative ion would lead to a decrease in the speed of interstitial diffusion. The fact that a diffusing species changes its ionic character is not unusual, copper has been found to be a negative ion at room temperature and a positive ion above 800°C in germanium[16]. Also independent electrical investigations indicate that gold normally exists as a positive ion in silicon at room temperature[17].

The interesting sign reversal of the gold ion mobility (Figure 8) is the basis for the entrainment theory. All the mobilities below 1600°K agree with the predictions of Fiks[8], but the two high temp-

erature measurements do not. There is no reason why these mobilities should agree as well as they do with the calculated values using the Einstein relationship. If the mean free path is taken to vary with temperature as l_o/T (as theory predicts) and the number of carriers depends on temperature in the well known way[11], equations (17) and (18) may be combined to give[8]

$$\mu_{eff} = \mu_o(T) \left\{1-A_o l_o \bar{\sigma}_o \left(\frac{T}{T_o}\right)^{3/2} \exp\left(-1.21/KT\right)\right\} \qquad (22)$$

where T_o is the reference temperature. This equation states that the effective mobility should continually increase (toward the anode) as temperature increases above 1600^oK.

Throughout the temperature range, Figure 9 shows that the mobility of vacancies remains relatively constant and proportional to the calculated Einstein value. It is interesting to note that if the charge on a vacancy is assumed to be in the region of +1 to +4, the equilibrium concentration of vacancies must be greater than or approximately equal to the equilibrium concentration of substitutionals which is not in agreement with the literature[2].

The relative solubility of both substitutional and interstitial gold in silicon is shown in Figure 10. Again the low temperature characteristics were taken from other sources[14], and the extension reproduced on the graph. The general shape of the total solubility agrees well with the results of Trumbore[14].

Why all these characteristics of the gold-silicon system deviate from their low temperature trends at approximately the same

temperature is difficult to explain under the ion entrainment theory.

If, in fact, the gold is in equilibrium as a negative ion at temperatures near the melting point of silicon, the behavior of both the gold and vacancy mobilities are readily explained, since they both are in agreement with Einstein's relationship. The larger size of the negative ion explains at least in part the decreased solubility of both substitutional and interstitial gold.

This decreased solubility by itself would tend to increase the observed vacancy controlled diffusion coefficient (equation 7).

$$D_{eff} = (C_v)_s \, D_v/((C_v)_s + (C_{sub})_s) \qquad (7)$$

The experimental data indicates the exact opposite occurs. This may be due to the negative substitutional ions attracting positive vacancies and tieing up vacancies such as to change the equilibrium constant (K in equation 2).

Although it appears difficult to come to a definite conclusion as to the reasons for the high temperature characteristics of the gold-silicon system, the data in this investigation leads to the conclusion that the cause of the observed phenomena is best explained by an ionic change of the gold.

V. APPENDICES

Appendix 1

Equipment and Apparatus

1. Furnace:

The furnace used for preheating was a Lindberg tube furnace Model #54032. Accessories:

a. Argon Gas Supply - Matheson Hi Purity

b. Gas Pressure Regulator

c. Flow Meter - Kontes Viz-Flo "150" Flowmeter

2. Power Supply

The power supply used in this investigation was a Sorensen Model DCR 20-125A and possesses the following characteristics:

a. Output Voltage - 0 to 20 Vdc

b. Output Current - 0 to 125 Adc

c. Constant Current Regulation - $\pm$ 125 mA

d. Constant Current Ripple - .5%

3. Potentiometer

A Leeds and Northrup Model 8686 Millivolt Potentiometer accurate to one microvolt was used for EMF measurements.

4. Balance

A Mettler Analytical Balance, Type H-15, capable of detecting variations of .1 milligram was used to weigh the samples.

5. Counting Equipment

A Hamner Electronics Company System was used for all radioactive counting, consisting of:

a. Amplifier - Model N302

b. High Voltage Power Supply - Model N4035

c. Timer - Model N850R

d. Decade Scaler - Model N276

e. Probe - Model A-18 with well type Scintillation crystal

6. Description of Silicon Crystals

The silicon crystals were purchased from Semiconductor Specialties Corporation. The crystals were:

1. Grown by the Czochralski method
2. Determined to vary in dislocation density between 200 etch pits per square centimeter and 2000 etch pits per square centimeter.
3. In excess of 50 ohm-cm resistivity.
4. Cut to rectangular solids of dimensions 0.5 cm $\pm$ .010 cm, 0.5 cm $\pm$ .010 cm, and 2.0 cm $\pm$ .012 cm.
5. Cut so the 0.5 cm x 0.5 cm surface contained a (111) crystallographic plane $\pm 2^{o}$.
6. Polished so the 0.5 cm x 0.5 cm surface had a mirror finish.

7. Lapping Device

Shirn et al.[12] have calculated the errors involved in the determination of diffusion coefficients by the radioactive

tracer technique due to the thickness of the slice and misalignment of the slice from the diffusion plane. The approximate solution in the case involved is:

$$\frac{1}{D_a} = \frac{1}{D}\left\{1 - \frac{(d^2 + s^2)}{24Dt}\right\} \qquad (1)$$

Where D_a is the apparent diffusion coefficient, S is the misalignment distance, i.e., the angle times the specimen width, and d is the slice width. Thus to reduce these errors, the slices must be thin and parallel to the original surface. The width of the slice is a compromise with the counting signal to noise ratio. The misalignment error can and should be reduced to as small a value as possible.

To this end, the device shown in Figure 3 was designed. The crystal is mounted in the shaft with Aremco Crystal bond adhesive with the surface perpendicular to the diffusion direction. Since the sliding surface of the base is machined perpendicular to the centerline of the shaft hole, the shaft and crystal can be rotated to eliminate any variation in grinding paper thickness. The hole in the base was bored so as to give the tightest slip fit with the shaft to eliminate any wobble.

Misalignment distances of a fraction of a micron are easily reached with this device.

8. Description of Gold Isotope

The radioactive gold was purchased from Tracer Lab. The standard certification on November 16, 1966 was:

1. Principal Radionuclide - Gold - 195
2. Current Half Life - 183 days
3. Chemical Form - Au^3 in HCl
4. Principal Activity per Gram of Solution - 56.3 $\mu c \pm 5\%$
5. Purity - No contaminates.
6. Mode of Decay - orbital electron capture and isomeric transition from upper to lower isomeric state to platinum - 195.
7. Decay Energies (only those used in this investigation) - 0.22 Mev and 0.32 Mev.

Appendix 2

Temperature Measurements

The tungsten vs. tungsten-rhenium thermocouple used for temperature measurements in this investigation was calibrated using a reference grade platinum vs. platinum-rhodium thermocouple purchased from Engelhard Industries, Inc. The silicon-platinum eutectic system prevented using the reference grade thermocouple directly. The platinum thermocouple wire was certified by the manufacturer to be calibrated to a standard traceable to the National Bureau of Standards.

It should be noted that the calibration of the thermocouple may change during use. The magnitude of the change depends upon the temperature, the length of time, and the condition under which it is used. Thermocouples of the type covered by the manufacturer's certificate are reliable within about 0.25% up to 1300^{o}C if used in a clean oxidizing atmosphere and not used for extended periods above 1300^{o}C.

Appendix 3

Error of Counting

Consideration must be made of the error involved in counting a certain number of random emissions from a sample above a normal background rate.[13] Background is the unavoidable counting rate measured without a sample in the counting chamber. This unavoidable background is due to cosmic rays and possibly by stray radiation from nearby radioactive material. Then the relative probable error in the number of counts originating from the sample is:

$$E(N-N_B) = \frac{67\sqrt{N+N_B}}{N-N_B} \quad \text{percent} \qquad (1)$$

Where N is the total number of pulses counted in a given time from a sample, N_B is the number of pulses counted in the same time with chamber empty.

This error is that which has a 50% probability of being exceeded. Three times this error ($\pm$ two standard deviations) has only a 4% probability of being exceeded. The determination of activity in sample section terminated when the 4% probability of error in the number of pulses in a reasonable time reached 25%.

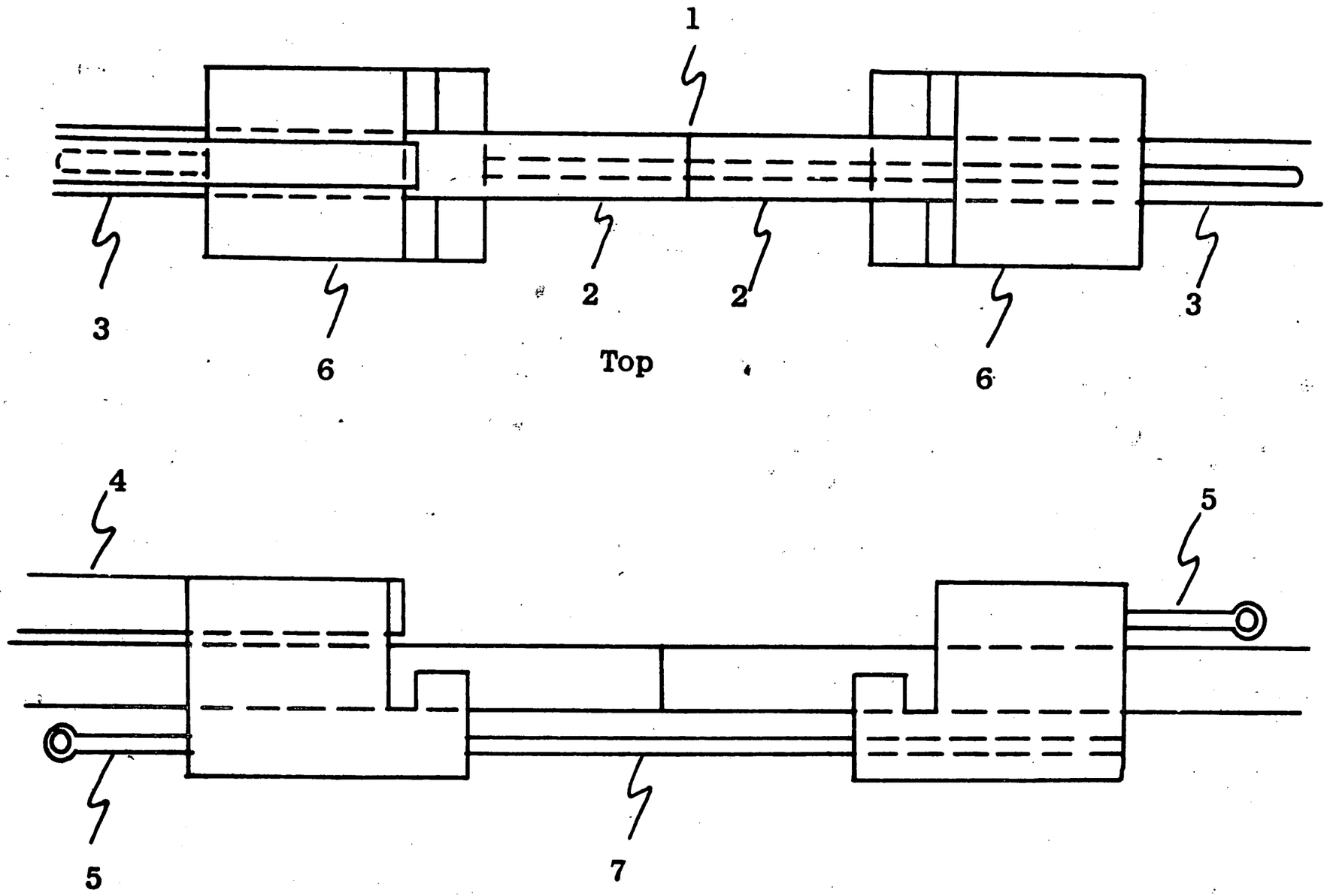

1. Radioactive gold interface
2. Silicon crystals
3. Tungsten electrodes
4. Alumina thermocouple guide
5. Holder withdrawal pins
6. Stainless steel holder
7. Guide and support

Figure 1. Schematic of crystal holder used to guide crystals into the furnace tube.

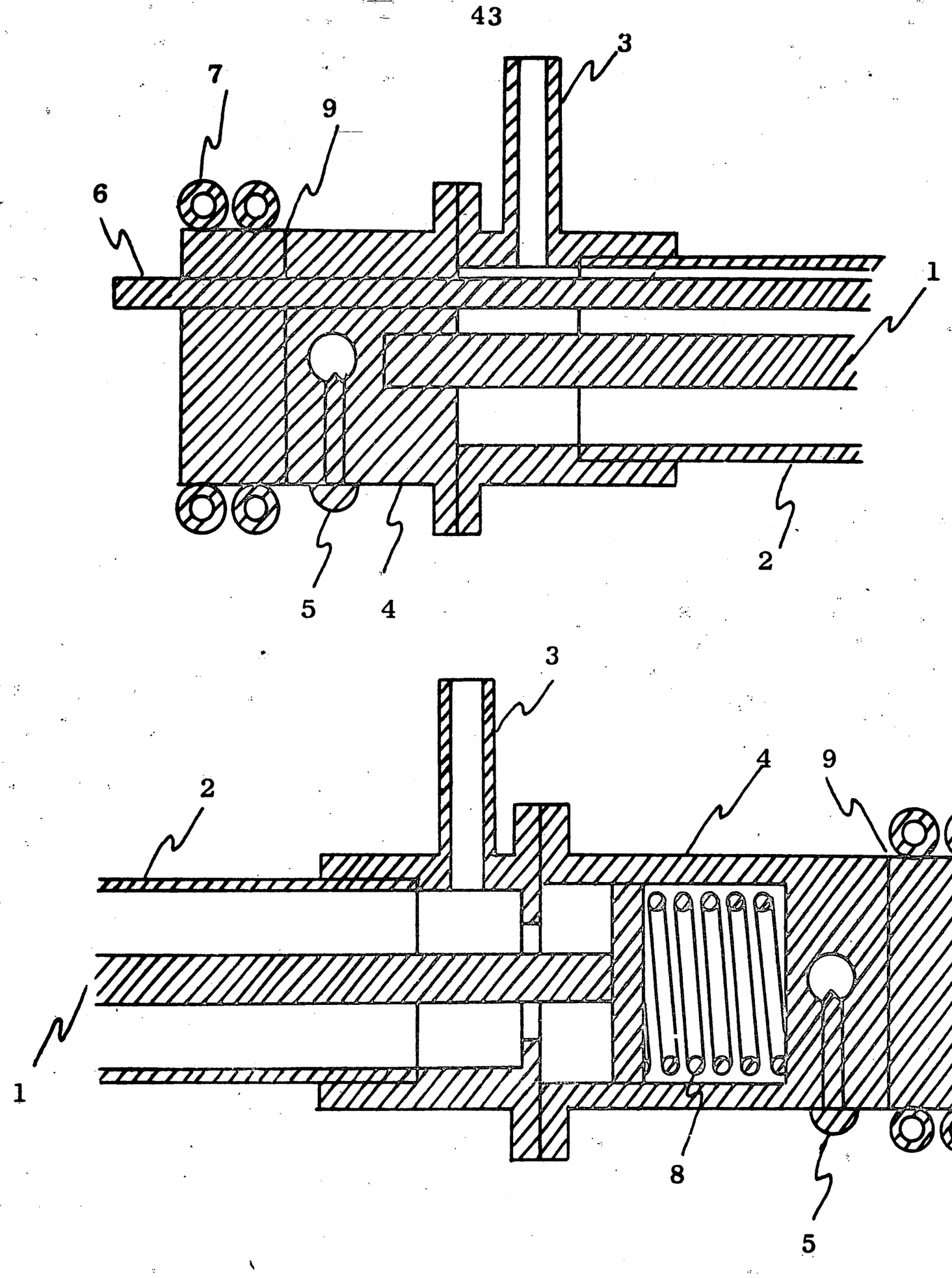

1. Tungsten electrode
2. Alumina tube (22 in. long)
3. Gas input or output
4. Aluminum end cap
5. Electrical connections
6. Alumina thermocouple guide
7. Water cooling tube and brass heatsink
8. Expansion spring
9. Mica electrical insulator

Figure 2. Schematic section of furnace tube end caps used as both electrodes and seals.

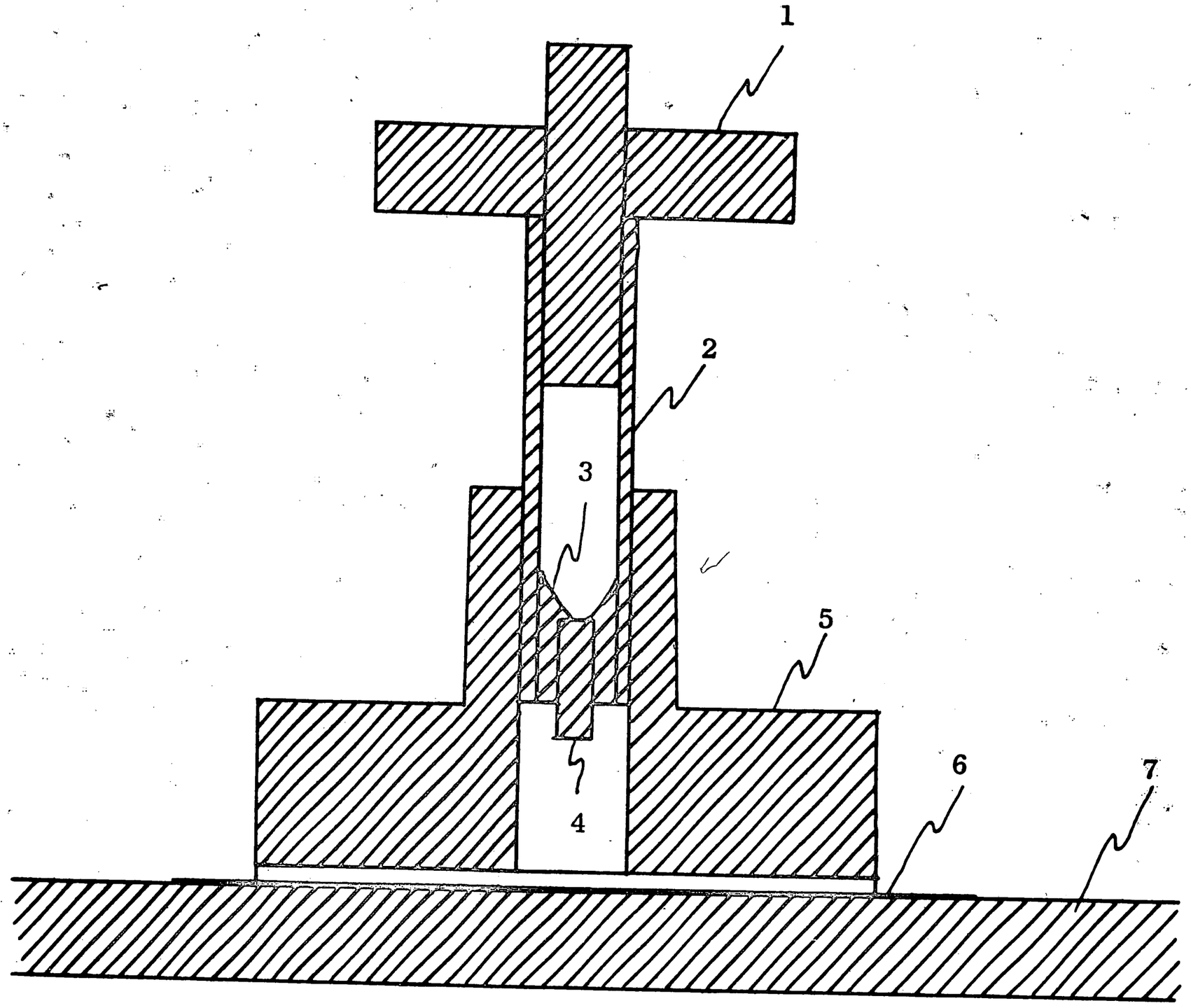

1. Weight
2. Crystal support
3. Thermoplastic cement
4. Crystal
5. Block for parallelism
6. Standard grinding paper
7. Flat block

Figure 3. Hand lapping crystal support used to maintain parallelism during removal of sections.

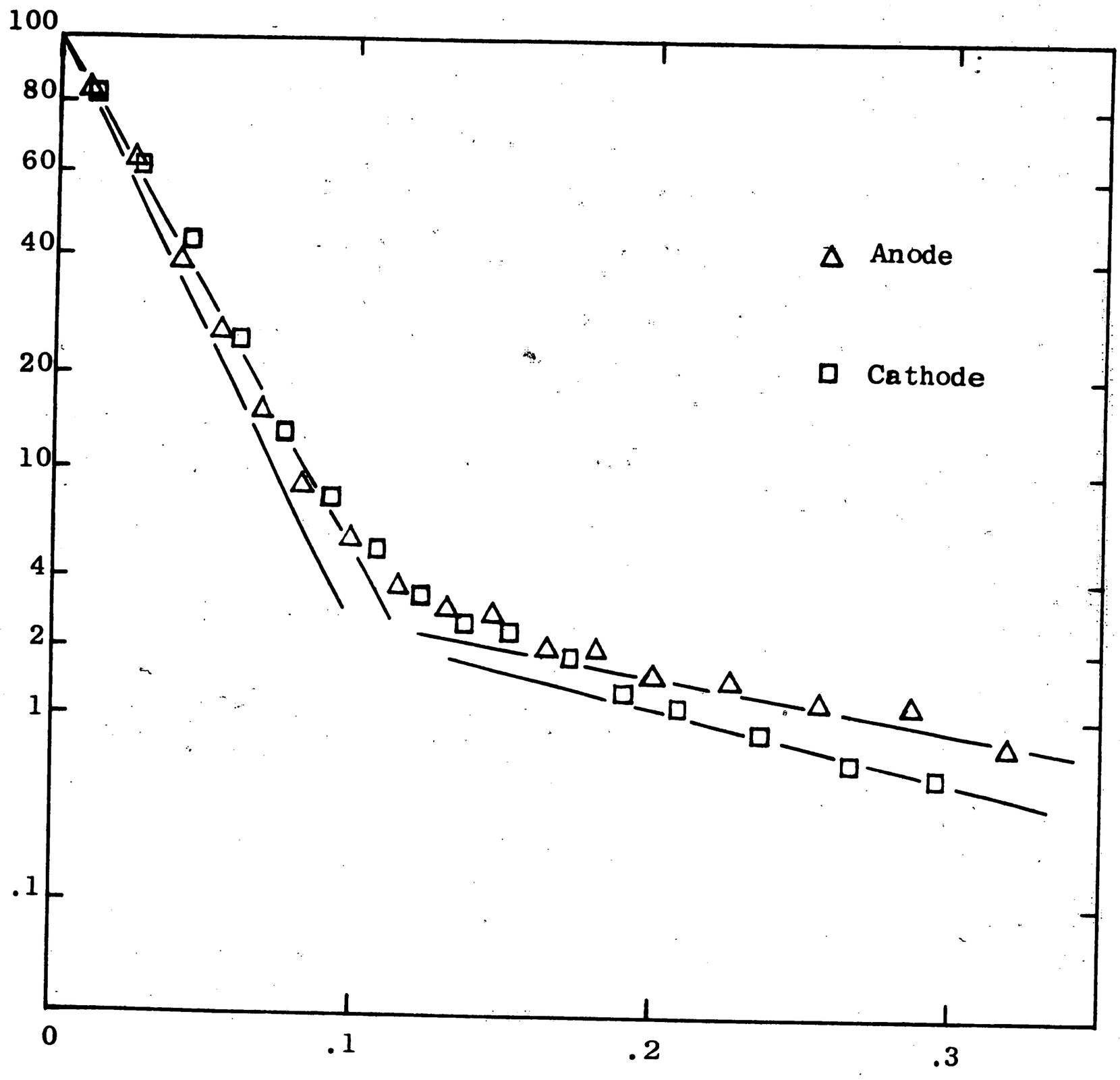

Figure 4. Distribution of gold diffused into silicon for 10 minutes at 1334°C (Probability Plot)

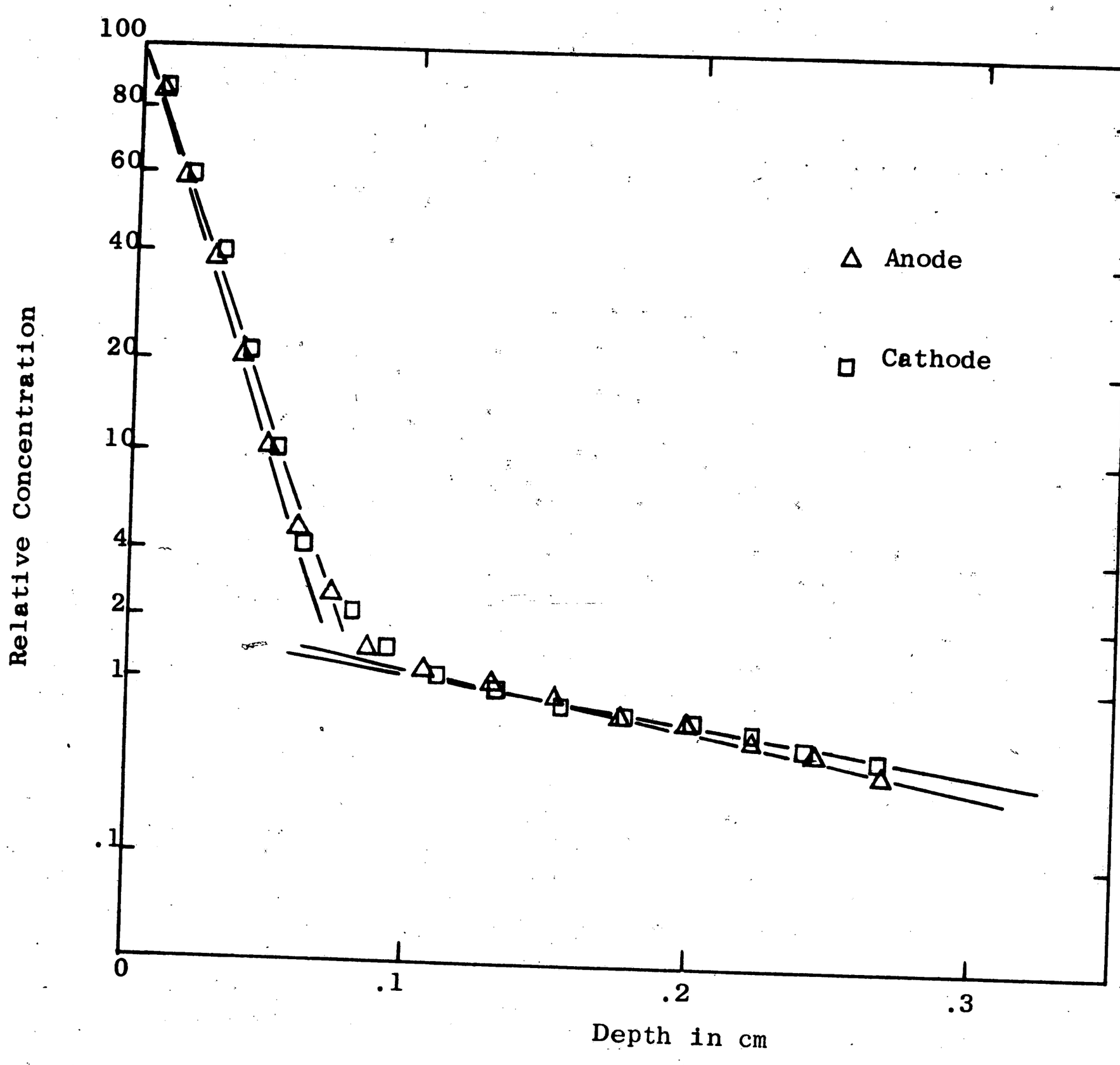

Figure 5. Distribution of gold diffused into silicon for 10 minutes at 1239°C (Probability Plot)

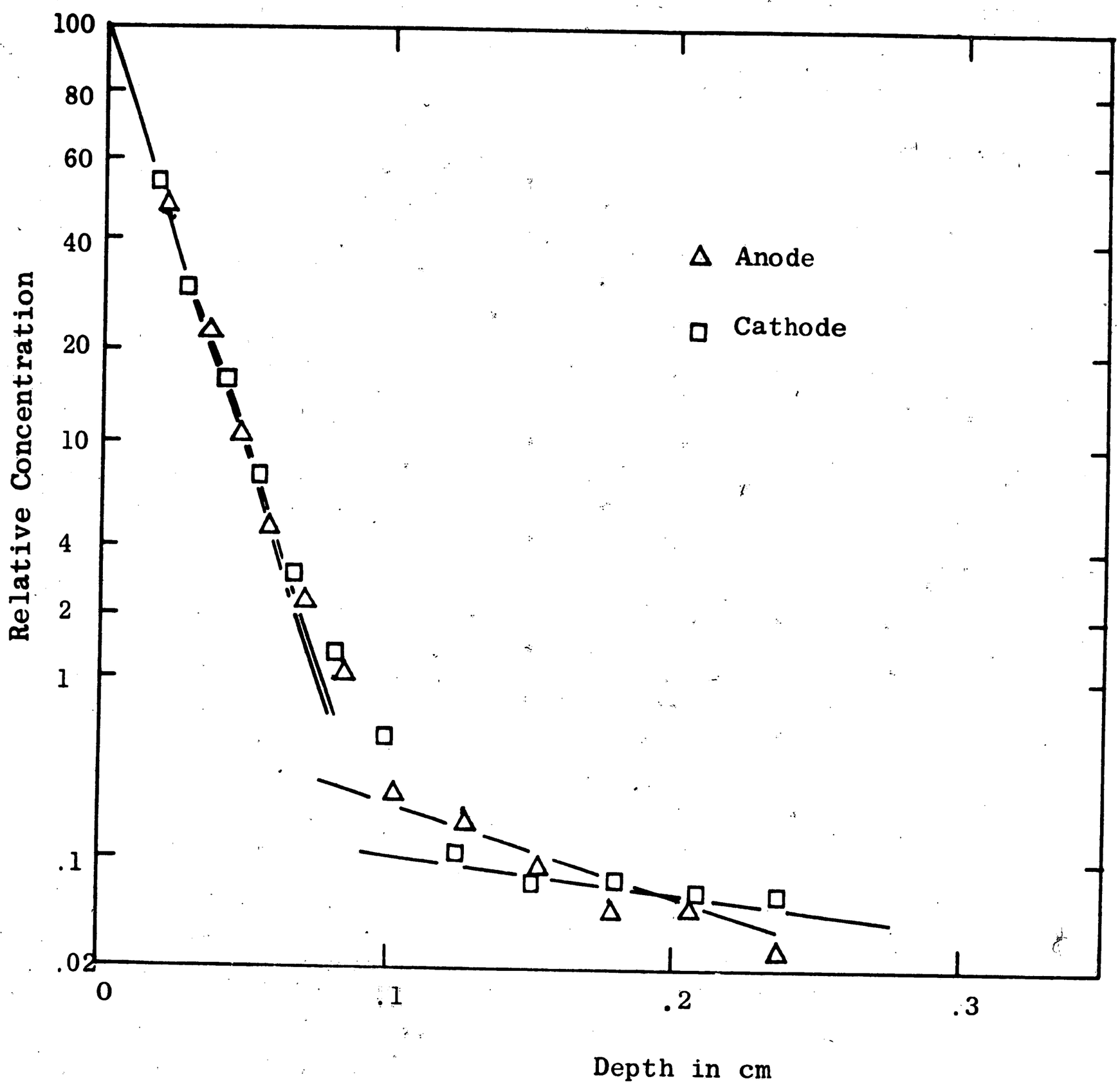

Figure 6. Distribution of gold diffused into silicon for 15 minutes at 1134°C (Probability Plot).

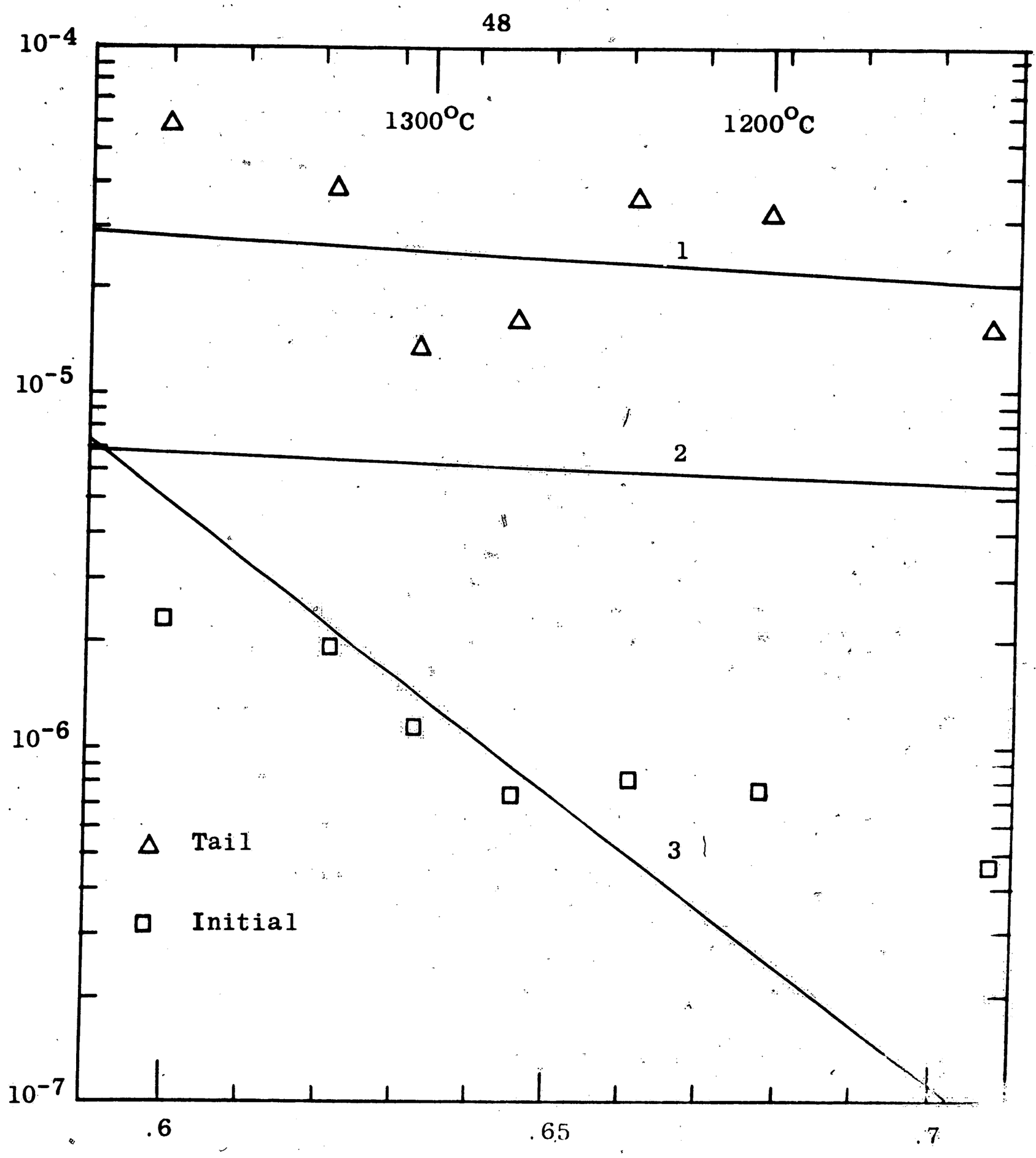

1. D (interstitial)^2
2. $C_i D$ (interstitial)$/C^2_{sub}$
3. $C_v D$ (vacancies)$/C^2_{sub}$

Figure 7. Diffusion coefficients of gold in silicon as a function of inverse temperature.

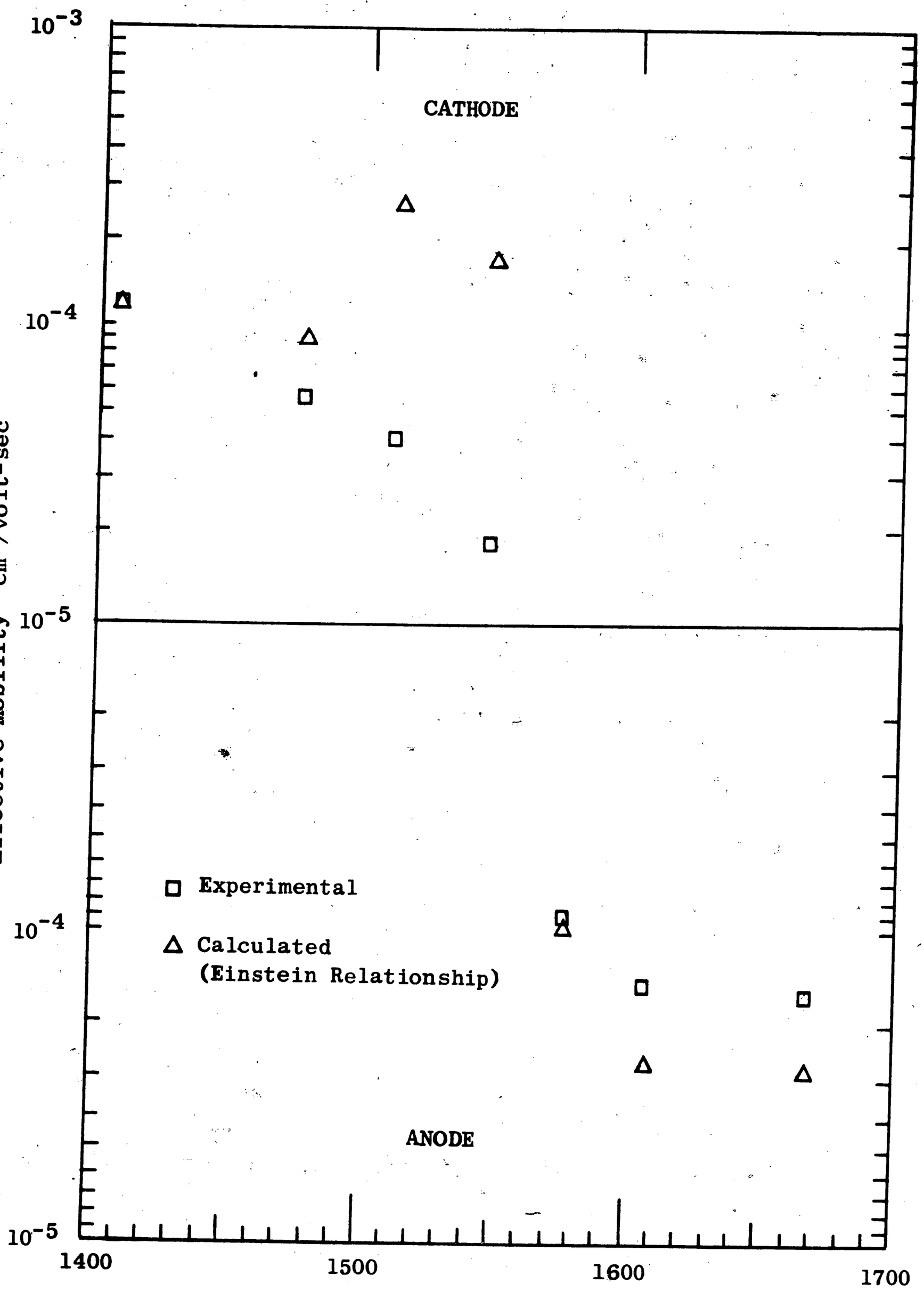

Figure 8. The temperature dependence of the effective mobility of gold in silicon.

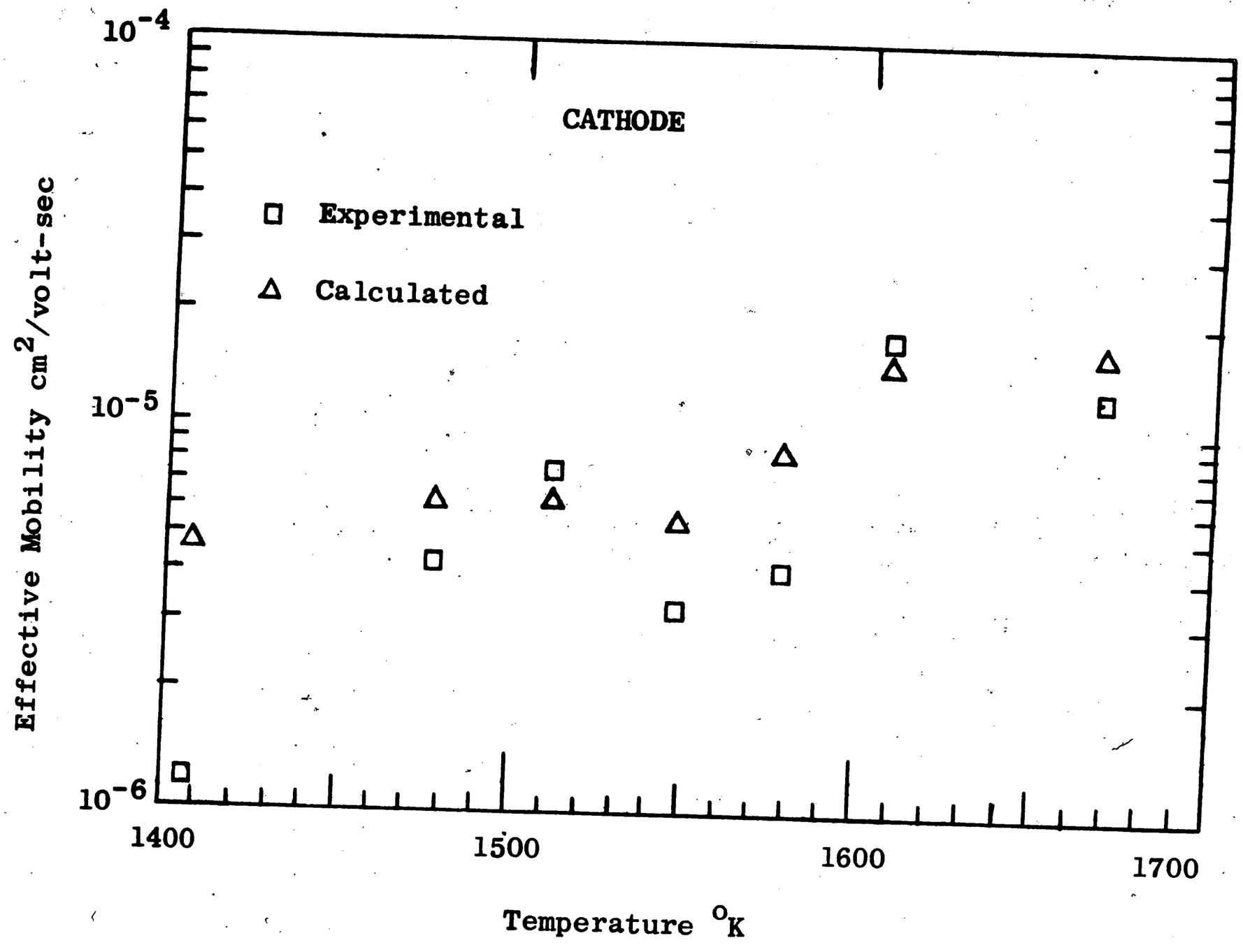

Figure 9. An indication of the temperature dependence of the effective mobility of vacancies in silicon.

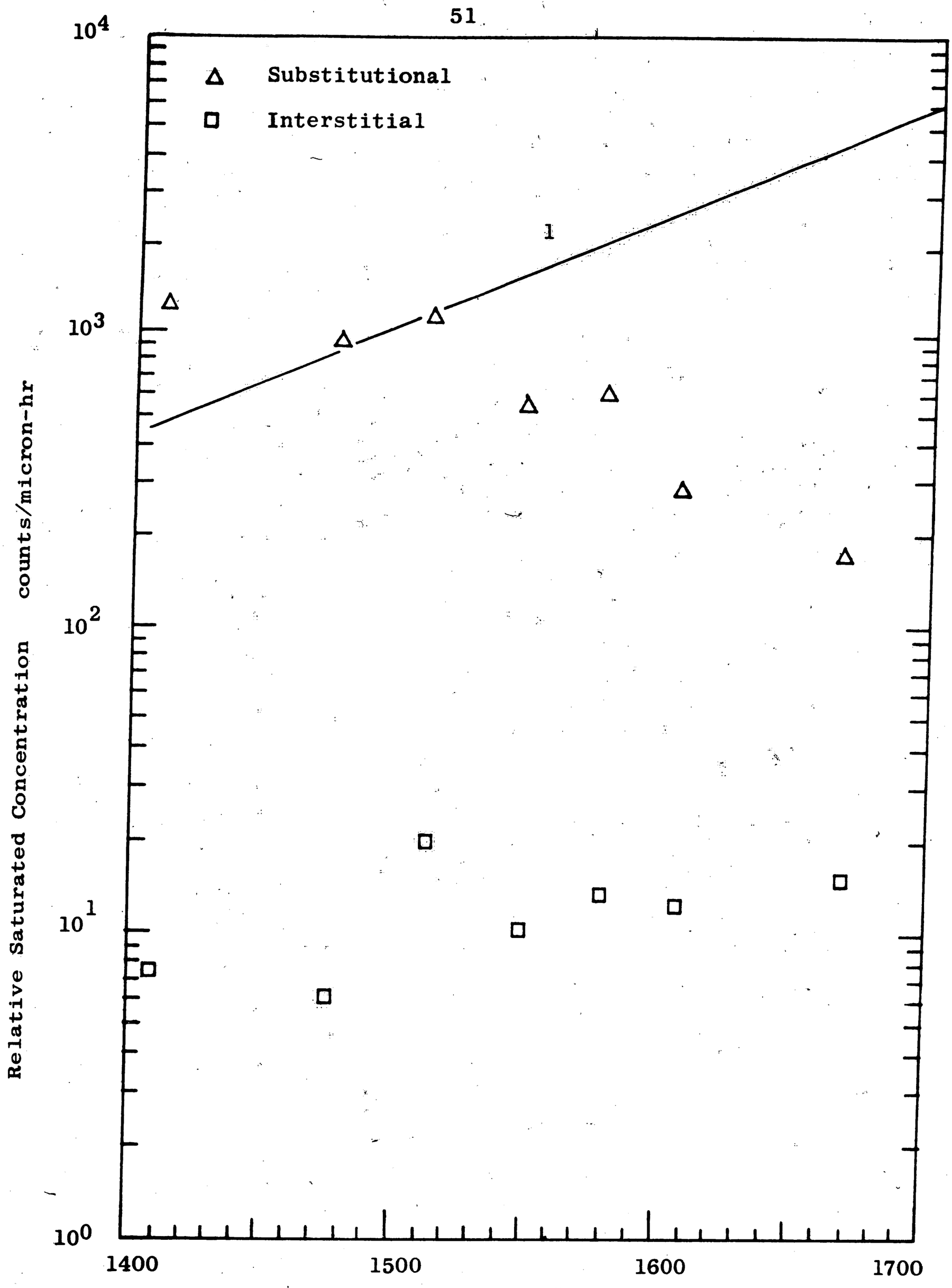

1. Extension of low temperature solubility[11]

Figure 10. The relative solubility of gold in silicon as experimentally determined from the intercept of the curves.

BIBLIOGRAPHY

1. Sprokel, G. J., "Interstitial-Substitutional Diffusion in a Finite Medium, Gold into Silicon," J. Electrochem. Soc. 112, 807-812 (1965).

2. Wilcox, W. R. and LaChapelle, T. J., "Mechanism of Gold Diffusion into Silicon," J. Appl. Phys. 35, 240-246 (1964).

3. Sprokel, G. J., and Fairfield, J. M., "Diffusion of Gold into Silicon Crystals," J. Electrochem. Soc. 112, 200-203 (1965).

4. Dash, W. C., "Gold-Induced Climb of Dislocations in Silicon," J. Appl. Phys. 31, 2275-2283 (1960).

5. Haeffner, E., "A Method of Changing the Isotope Abundance in Mercury," Nature 172, 775-776 (1953).

6. Skaupy, Z., Phsik. Chem. 58, 560 (1907).

7. Fiks, V. B., "On the Mechanism of the Mobility of Ions in Metals," Soviet Phys. - Solid State 1, 14-28 (1959).

8. Fiks, V. B., "Entrainment of Ion by Electrons in Semiconductors," Soviet Phys. - Solid State 1, 1212-1214 (1960).

9. Brooke, H., Advances Electronics and Electron Phys. 7, 85-182 (1955).

10. Boltaks, B. I., Kulikou, G. S. and Malkovich, R. Sh., "Electrical Transport of Gold in Silicon," Soviet Phys. - Solid State 2, 2134-2137 (1961).

11. Runyan, W. R., Silicon Semiconductor Technology (McGraw-Hill Book Company, New York, N. Y., 1965) p. 168 and 266.

12. Shirn, G. A., Wajda, E. S. and Huntington, H. B., "Self-Diffusion in Zinc," Acta Met. 1, 513-518 (1953).

13. Cullity, B. D., Elements of X-ray Diffraction (Addison-Wesley Publishing Company, Inc., Reading, Mass., 1959) p. 204-206.

14. Trumbore, F. A., "Solid Solubitities of Impurity Elements in Germanium and Silicon," Bell System Tech. J., 39 205-233 (1960).

BIBLIOGRAPHY (cont'd)

15. Adler, R. B., A. C. Smith, and R. L. Longini, Introduction to Semiconductor Physics (John Wiley and Sons, Inc., New York, N. Y., 1964), p. 35.

16. Boltaks, B. I., Diffusion in Semiconductors (Academic Press, New York, N. Y., 1963), p. 173.

17. Dunlap, W. C., Jr., An Introduction to Semiconductors (John Wiley and Sons, Inc., New York, N. Y., 1957), p. 273.

VITA

Roger Deane Peterson was born on October 31, 1933 in Minneapolis, Minnesota and is the son of Lloyd and Pearl Peterson. He is a graduate of Central High School of Sheboygan, Wisconsin.

After graduation he became a member of the United States Air Force from which he retired in January, 1958 as a reserve officer. He received his Bachelor of Science in Electrical Engineering from the University of Wisconsin in August, 1961.

In September, 1961 he began employment with the Western Electric Company at Murray Hill, New Jersey as a Development Engineer in Satellite Communication Ground Stations. Since July, 1965, he has been a Lehigh Master's candidate at the Engineering Research Center (Western Electric - Princeton), where he has been working on radioisotope applications.

He is a member of Eta Kappa Nu and Tau Beta Pi.